A Rhesus Monkey With a Naturally Occurring Impairment of Disparity Vergence. II. Abnormal Near Response Cell Activity in the Supraoculomotor Area

Mark M. G. Walton,[1] Adam Pallus,[1,2] and Michael Mustari[1–3]

[1]Washington National Primate Research Center, University of Washington, Seattle, Washington, United States
[2]Department of Ophthalmology, University of Washington, Seattle, Washington, United States
[3]Department of Biological Structure, University of Washington, Seattle, Washington, United States

PURPOSE. Convergence insufficiency is a very common disorder that can have significant adverse effects on school performance. When reading, children with this disorder often experience diplopia and headaches. We have recently obtained a rhesus monkey with a naturally occurring impairment of vergence eye movements. In the companion paper, we report behavioral testing that shows a pattern of impairments similar to what clinicians observe in human children with convergence insufficiency, including a receded near point, an exophoria that increases as target distance decreases, and difficulty maintaining an appropriate vergence angle when presented with a large field stimulus at near. For the present case report, we wondered whether these behavioral deficits would be associated with abnormal discharge patterns in brainstem neurons related to vergence eye movements.

METHODS. Single unit activity was recorded from near and far response cells in the supraoculomotor area in the vergence-impaired monkey, while he performed a smooth vergence tracking task or fixated visual targets at different distances.

RESULTS. We found an abnormally weak sensitivity to both vergence angle and vergence velocity. Nonetheless, these neurons modulated in association with contextually inappropriate slow vergence movements that occurred in the absence of saccades but not for slow divergence drifts that immediately followed converging saccades. Modulation of activity was more robust when additional depth cues were available.

CONCLUSIONS. These data suggest that disorders affecting vergence eye movements may be associated with impoverished sensory input to the near and far response cells and, perhaps, aberrant tuning in vergence-related neurons.

Keywords: convergence insufficiency, supraoculomotor area, near response, vergence, monkey

Vergence eye movements are crucial for many everyday tasks, such as computer use and reading. Disorders that affect these movements, such as convergence insufficiency (CI), can have a profound impact on a person's quality of life. The exact prevalence of CI is somewhat uncertain, but the available literature suggests a prevalence of 2% to 17%.[1] Children with CI often experience diplopia, headaches, and blurry vision when performing close work.

In the companion paper, we report the results of behavioral tests on a rhesus monkey with a naturally occurring impairment of vergence eye movements (monkey CI). We wondered whether this animal would show abnormalities in brainstem regions that play a role in the generation of vergence eye movements. An ideal target for such a study is the supra-oculomotor area (SOA). This structure, located dorsal and lateral to oculomotor nucleus, contains near and far response cells.[2,3] These neurons exhibit tonic discharge that is strongly related to vergence angle and/or a transient increase in firing rate that is correlated with vergence velocity.[4–7] In the present case report, we present the results of single-unit recordings of near and far response cells in SOA of the same vergence-impaired monkey used for the companion paper (monkey CI). Results are compared to those obtained from normal monkeys performing vergence tasks in a previous study.[5]

METHODS

Subjects and Surgical Procedures

Subject CI was a rhesus macaque monkey (*Macaca mulatta*) that showed a receded near point of convergence, reduced gain of vergence pursuit of a target moving in depth, and a consistent exodeviation when fixating targets at near. Neurophysiologic data from this animal were compared to those obtained from normal monkeys (N1 and N2) for a recently published paper that used the saccade-vergence task.[8]

All procedures were performed in compliance with the National Institutes of Health Guide for the Care and Use of Laboratory Animals and the ARVO Statement for the Use of Animals in Ophthalmic and Vision Research. The experimental protocol was reviewed and approved by the Institutional Animal Care and Use Committee at the University of

Investigative Ophthalmology & Visual Science

Washington. Detailed descriptions of the surgical procedures can be found in previously published work.[9-11] The neurophysiologic studies described in this report required two sterile surgeries. In the first, a titanium head post (Crist Instruments Co., Inc., Hagerstown, MD, USA) was permanently attached to the skull so that the head could be restrained during experiments. In the same surgery, eye coils were chronically implanted underneath the conjunctiva of both eyes.[12,13] Following this, the monkey was trained on a target step saccade task (see below) until he attained proficiency. Then, in a second surgery, titanium recording chamber was affixed to the skull over a 16-mm craniotomy.

Behavioral Tasks and Visual Display

For the duration of all recording sessions, the monkey sat in a primate chair, with the head restrained, at the center of a 1.5-m magnetic coil frame. Monkeys were initially trained to fixate a 0.25° laser spot that stepped to various locations on a tangent screen situated 57 cm from the eyes (Target Step Saccade Task, see companion paper). Target locations were chosen by randomly selecting horizontal and vertical coordinates (−20° to 20°, in 2° increments). This task reliably elicits a saccadic eye movement each time the target moves. After monkey CI had been proficient at this task for more than 6 months, we introduced the following tasks that required vergence eye movements.

Saccade-Vergence Task. This task is essentially the same as the target step saccade task, except that the visual targets consisted of 60 red, plus-shaped LEDs positioned in various horizontal and vertical directions, at 12 distances (10.2 cm, 11.0 cm, 11.9 cm, 13.1 cm, 14.4 cm, 16.0 cm, 18.1 cm, 20.7 cm, 24.2 cm, 29.0 cm, 36.3 cm, and 48.5 cm) in three-dimensional space (see companion paper for a schematic illustration). Because far targets could be either up or down, this task allows us to dissociate vertical eye position and target distance. The monkey was rewarded for keeping both eyes within 2° imaginary windows around the "ideal" eye position. For near targets, of course, this required that the eyes point in different directions (convergence). The ideal vergence angle was computed based on the distance of the target in three-dimensional space and the monkey's interpupillary distance. Due to monkey CI's difficulties with this task (see companion paper), it was used sparingly for the present neurophysiologic study. This was the only behavioral task used for two neurons but, for most recordings, other tasks were used.

Near Fixation Task. A black and white random checkerboard pattern, 14 × 14 cm, was positioned at a distance of 10 cm, directly in front of the monkey's face. Individual elements of the pattern were approximately 5 × 5 mm, but because they were randomly arranged, groupings of same-color elements formed some larger shapes (up to 30 mm wide). The monkey viewed this stimulus pattern in a lighted room and was rewarded for fixating on any part of the pattern, as long as he maintained convergence of at least 10°. This task was designed to provide a rich disparity and accommodative stimulus to help monkey CI to achieve a large enough convergence angle to estimate the vergence position sensitivities of near and far response neurons. Because monkey CI had difficulty maintaining a consistent, appropriate vergence angle during this task, this elicited a wide range of vergence angles and permitted analysis of changes in firing rate associated with this vergence instability. This task also allowed an analysis of changes in the firing rates of near and far response cells when the monkey failed to maintain the appropriate vergence angle, under conditions that were at least somewhat similar to what a human child with CI might experience when reading.

Smooth Vergence Tracking Task. A 3.5-mm red, plus-shaped LED was mounted on a movable platform, controlled by a high precision linear motion actuator (Zaber Technologies Inc., Vancouver, BC, Canada). To elicit smooth, symmetric vergence tracking, the direction of motion was aligned with the monkey's midsagittal plane. The target always moved at a constant velocity (triangle wave, frequency 0.05–0.2 Hz). For some experiments, the target was surrounded on three sides by a 15 × 15-cm black and white checkerboard pattern. In this latter case, the room was dimly illuminated so that the monkey would be able to see the pattern.

Unit Recording and Localization of SOA

Tungsten and glass microelectrodes (Frederick Haer, Bruswick, ME, USA) were used to record the extracellular activity of isolated neurons from the SOA, immediately dorsal and lateral to oculomotor nucleus.[2-4,8] SOA was identified based on the presence of tonic neural activity related to vergence angle, the occurrence of symmetrical vergence eye movements in response to microstimulation, and proximity to well-known landmarks, such as oculomotor nucleus. When searching for neurons, we used either the smooth vergence tracking task or the near fixation task. In the latter case, the variation in vergence angle needed to identify SOA neurons was achieved due to the animal's inability to maintain a stable convergence appropriate to the target distance.

Data Analysis

Data acquisition and preliminary analyses were conducted using Spike 2 software (Cambridge Electronic Design, Cambridge, UK). All data were then imported into Matlab (Mathworks, Natick, MA, USA) for quantitative analyses using custom functions. Offline spike detection was conducted using the same custom algorithm used in previous studies.[14,15]

The instantaneous horizontal and vertical velocities were estimated for both eyes using 7-point parabolic differentiation of the eye position signals. Saccades were detected using a custom algorithm based on a combination of velocity and acceleration criteria.[16] Vergence angle was computed using Equation 1:

$$Verg = H_{Left} - H_{Right} \qquad (1)$$

where Verg, H_{Left}, and H_{Right} represent vergence angle, horizontal left eye position, and horizontal right eye position, respectively.

Similarly, vergence velocity was computed using Equation 2:

$$\dot{V}erg = \dot{H}_{Left} - \dot{H}_{Right} \qquad (2)$$

where $\dot{V}erg$, $\dot{H}_{Left}$, and $\dot{H}_{Right}$ represent vergence velocity, horizontal left eye velocity, and horizontal right eye velocity, respectively. Saccade onsets were identified using an algorithm based on vectorial eye velocity and acceleration, described in detail in the companion paper.

The onsets of periods of steady fixation were detected, based on the following criteria: (1) No saccades were detected within the preceding 100 ms; (2) vergence velocity was below 10°/s, (3) the duration of the identified period of fixation was at least 500 ms, and (4) the monkey was looking in the direction of the checkerboard stimulus. In addition, all periods of steady fixation ended at least 10 ms before the onset of the next saccade. The relationship between the vergence angle and the mean firing rate during these periods of steady fixation was assessed using linear regression analysis.

Many neurons in SOA carry signals related to vergence velocity, in addition to vergence position.[4,8] Vergence-only

movements, defined as those occurring in the absence of detectable saccades, were detected using an algorithm described in the companion paper. To estimate the portion of the firing rate associated with vergence velocity, the firing rate predicted on the basis of mean vergence angle was subtracted from the observed mean firing rate during vergence-only movements that occurred during the performance of the near fixation task, according to Equation 3:

$$FR_{V\dot{e}rg} = FR_{Observed} - FR_{Static} \qquad (3)$$

where FR_{Static} is the predicted mean firing rate based on vergence position (derived from linear fits to the static vergence rate-position curve) and $FR_{Observed}$ is the actual mean firing rate during each vergence-only movement. $FR_{V\dot{e}rg}$, then, is the portion of the firing rate that we predicted would be specifically related to vergence velocity. Note that $FR_{V\dot{e}rg}$ can be negative if the mean firing rate is lower than what would be expected based on the neuron's vergence position sensitivity. A linear regression analysis was then performed to determine whether $FR_{V\dot{e}rg}$ was related to mean vergence velocity during vergence-only movements.

The vergence velocity sensitivity was also assessed during saccades (many of which were disjunctive) and vergence drift (see companion paper) during performance of the near fixation task by fitting the data with a dynamic equation (Equation 4) that included terms for vergence position and velocity[8]:

$$FR(t) = a + k_{Verg}V(t + t_d) + r_{Verg}\dot{V}(t + t_d) \qquad (4)$$

where k_{Verg} and r_{Verg} represent the sensitivity to vergence position and velocity, respectively. The expression $(t + t_d)$ represents a time shift to compensate for neural processing delays. As we have done in two other recent studies, we used a time shift of 20 ms for all neurons.[5,8] Data obtained during performance of the smooth vergence tracking task were also fit with Equation 4. For each recording, model performance (measured by the R^2 value) was evaluated by using the first half of the data to obtain parameter estimates, which were then used to predict the instantaneous firing rates for the second half of the data.

RESULTS

A detailed analysis of monkey CI's performance on tasks requiring vergence can be found in the companion paper.

Single-unit recordings were obtained from 43 neurons from monkey CI. For 28 of these, the near fixation task was used. The remaining 15 neurons were recorded while the monkey performed the smooth vergence tracking task. Overall, 14/43 neurons (33%) recorded from monkey CI were classified as far response cells.

Near Fixation Task

Figure 1 shows raw data from a near response cell (A) and a far response cell (B), recorded from monkey CI1 during performance of the near fixation task. Both neurons show a robust modulation with vergence angle. The animal's obvious difficulties associated with maintenance of the appropriate vergence angle are clearly associated with decreased activity from the near response cell and increased activity from the far response cell. This same pattern was consistently observed across the neurons recorded during performance of the near fixation task. This variability in firing rate and vergence angle permitted statistical analysis of the vergence position sensitivities of neurons recorded from monkey CI, despite the animal's

difficulties with vergence tasks. One of the 28 neurons recorded during performance of the saccade-vergence and near fixation tasks showed a transient discharge related to vergence velocity, but no tonic discharge associated with vergence position. This neuron was excluded from analyses of vergence position sensitivity.

Figure 2 shows vergence rate-position curves for two example neurons, including one with a slope close to the mean for monkey N1 and one with a slope close to the mean for monkey CI1. For both example neurons, the R^2 values were higher than the mean (but were well below the maximum) for that animal. For both neurons, the tonic firing rates were significantly correlated with vergence angle, but the slopes and R^2 values were notably lower for the neuron recorded from monkey CI. These effects were typical for both near and far response cells. The absolute values of the slopes were significantly larger for normal monkeys, compared to monkey CI (normal, 5.36; CI, 3.13; $P = 0.003$). The R^2 values were also significantly greater for the normal monkeys (normal, 0.49; CI, 0.21; $P < 0.0001$, two-tailed t-test).

Figure 1 suggests that the contextually inappropriate divergence observed during performance of the near fixation task may be associated with decreased firing rates of near response cells and increased firing rates of far response cells. To explore this possibility quantitatively, periods of intersaccadic vergence were identified using the procedures described in the companion paper; the resulting data were then fit with Equation 4. Figure 3 shows the resulting parameter estimates for vergence position and velocity and the R^2 values. The vergence position term was significantly different from zero for 25/27 neurons, with a mean absolute value of 2.61. The vergence velocity term was significantly different from zero for 20/27 neurons, with a mean absolute value of 0.31. The R^2 values were good for some neurons (green and yellow dots) but tended to be poor overall (mean, 0.12), compared to what we recently reported when we used the same equation to analyze vergence movements without saccades in normal monkeys (mean, 0.39).[8]

The above analysis indicates that, in monkey CI, contextually inappropriate vergence movements (i.e., during fixation of a large-field stimulus at near) were associated with modulation of activity in near and far response cells. From an examination of Figure 1, one can see that changes in vergence angle included disjunctive saccades, slow vergence drifts after saccades, and vergence-only movements. The vergence drifts that immediately follow saccades in this animal might not be the same phenomenon as vergence-only movements (which are often voluntary). For example, in the companion paper we saw that converging saccades were often followed by inappropriate slow divergence. We wondered whether these postsaccadic slow vergence drifts were encoded by SOA neurons, particularly those that carry signals related to vergence velocity. If so, then $FR_{V\dot{e}rg}$ (derived from Equation 3, see Methods) should be correlated with postsaccadic vergence velocity for a subset of SOA neurons. As a first step, to identify neurons that encode vergence velocity, we analyzed the relationship between mean vergence velocity and mean $FR_{V\dot{e}rg}$ for vergence-only movements, using linear regression. This analysis was only performed for a given neuron if at least seven such movements were detected. Because most slow vergence movements are accompanied by one or more saccades, it is somewhat difficult to obtain a large number of these movements for a given recording. Thus, eight neurons were rejected for failing to meet the above criterion. The distributions of the slopes and R^2 values for this analysis are shown in panels A and B, respectively, of Figure 4 for the remaining 20 neurons. The slope was significantly different from zero for 9/20 neurons (45%) and the R^2 value exceeded
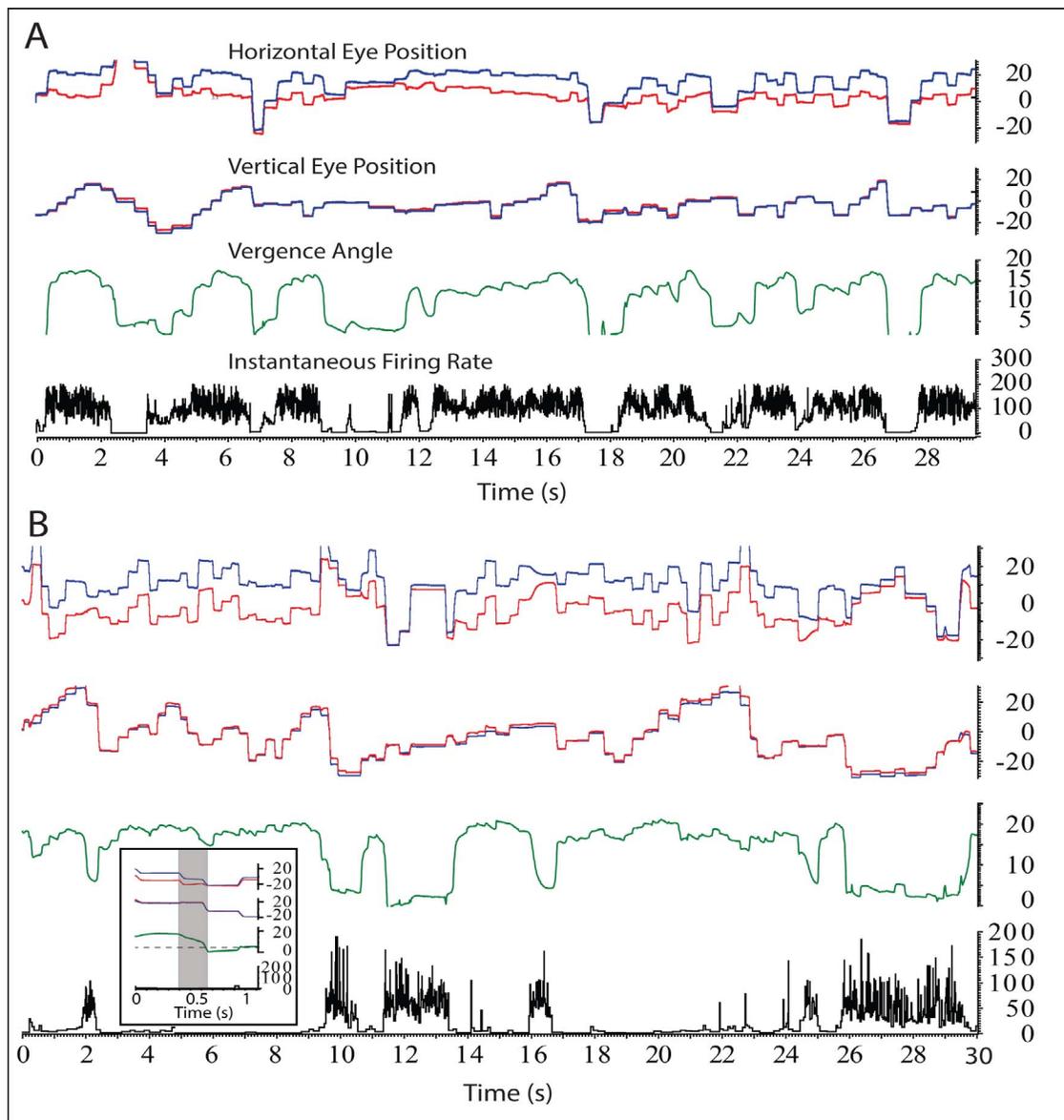
FIGURE 1. Thirty seconds of raw data for two example neurons, recorded while monkey CI performed the near fixation task, including a near response cell (**A**) and a far response cell (**B**). Sudden, large reductions in the vergence angle were consistently associated with large decreases in the tonic firing rate of the near response cell and large increases in the firing rate of the far response cell. The inset shows a large divergence associated with saccades. The *gray shaded area* highlights a conjugate saccade followed by a slow divergence drift, followed by a diverging saccade. The *dashed line* indicates a vergence angle of 5°. Note that there is no discharge from the neuron, even though the vergence angle ends up being <5°.

0.2 for 9/20 neurons (panel B). When the same analysis was performed on the vergence drifts that immediately followed saccades, however, the R^2 values were below 0.05 for all 20 neurons (panel B). The inset of Figure 4B shows examples of this analysis for the neuron with the strongest correlation for vergence-only movements. Note that, although this neuron convincingly encoded vergence velocity during vergence-only movements (left), there was no relationship for slow post-saccadic vergence drifts (right).

For the example neuron shown in Figure 4B $FR_{Vèrg}$ was negative for divergence-only movements. Thus, the vergence velocity signal for this neuron involves both an enhancement of firing rate for ongoing convergence and a decrement in firing rate for ongoing divergence. Overall, there were 12 neurons with at least 7 off-direction vergence-only movements (all were near response cells, presumably because vergence-

only movements were most likely to happen when monkey CI inappropriately diverged). The mean $FR_{Vèrg}$ (averaged across all off-direction vergence-only movements) was negative for all 12 of these neurons (overall mean, −30.3 spikes/s).

Smooth Vergence Tracking Task

In the companion paper, we saw that monkey CI was unable to converge more than ∼5° to 6° when the only available stimulus was a 1° red plus-shaped target but was able to achieve a vergence angle of more than 15° when presented with a large-field random checkerboard pattern. Presumably, the improved performance was due to the much richer disparity and accommodative information present in the latter task. In the analyses above, however, we saw that the vergence position and velocity sensitivities of SOA neurons were still not normal
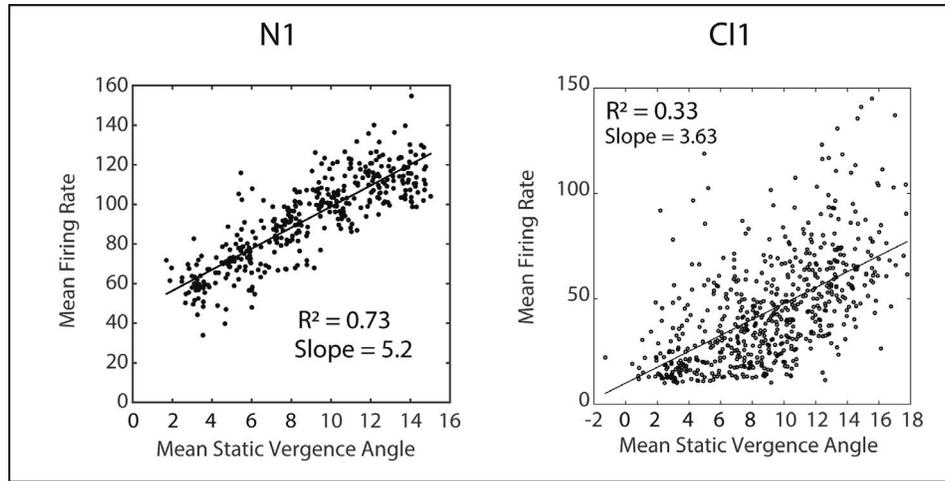
FIGURE 2. Example vergence rate-position curves for two typical example neurons, including one from a normal monkey (N1) and one from monkey CI. Note that the slope was notably larger for the neuron recorded from the normal animal and the R^2 value was considerably larger.

for the near fixation task. When an object is approaching an observer, additional depth cues become available, such as looming and radial optic flow; these monocular depth cues can elicit vergence eye movements at short latencies.[17-19] Monkey CI was able to perform the smooth vergence tracking task when the target was surrounded by the random checkerboard pattern. We wondered, therefore, whether the rich array of depth cues available in this latter version of the task might be associated with larger vergence position and velocity sensitivities of SOA neurons. With these considerations in mind, 15 neurons were recorded during performance of the smooth vergence tracking task. Four of these, however, were recorded
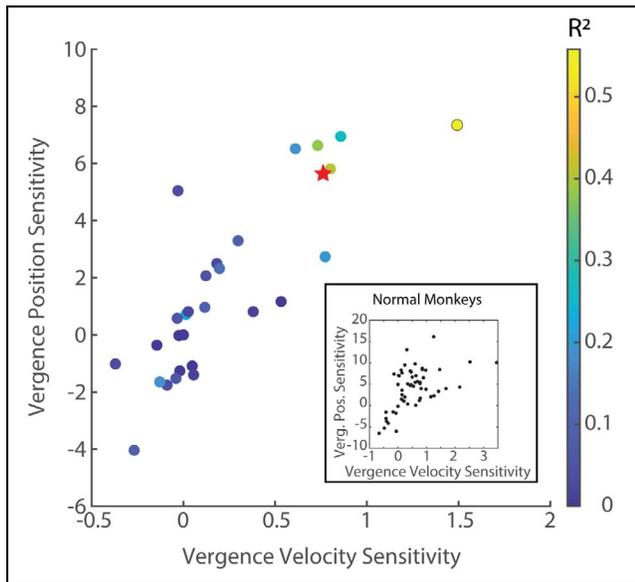

FIGURE 3. Estimated sensitivities to vergence position and velocity for monkey CI, derived from dynamic model fits to vergence movements that occurred between saccades during performance of the near fixation task. The color of each dot represents the R^2 value. The *inset* shows this comparison for normal monkeys, using data replotted from Pallus et al.[8] Note that the data in the *inset* are plotted on a different scale because the sensitivities were much larger for normal monkeys. The *red star* in the main plot indicates the mean position and velocity sensitivities for normal monkeys.
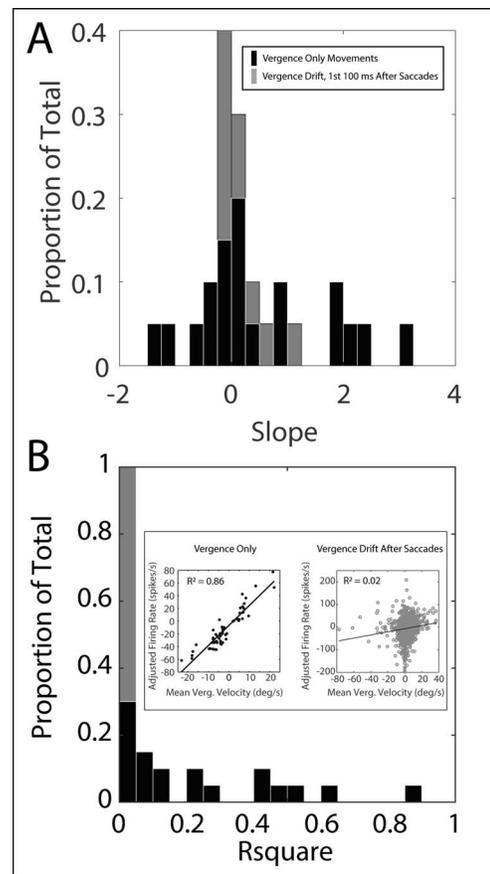

FIGURE 4. Comparison of slopes (**A**) and R^2 values (**B**) derived from linear regression analysis of the relationship between FR_{verg} (see Methods) and vergence velocity, for vergence-only movements (*black bars*) and slow vergence drifts that immediately followed saccades (*gray bars*). Both the slopes and the R^2 values tended to be near zero for postsaccadic vergence drifts, even for neurons that showed a robust sensitivity to vergence velocity during vergence-only movements (see inset in panel **B**).
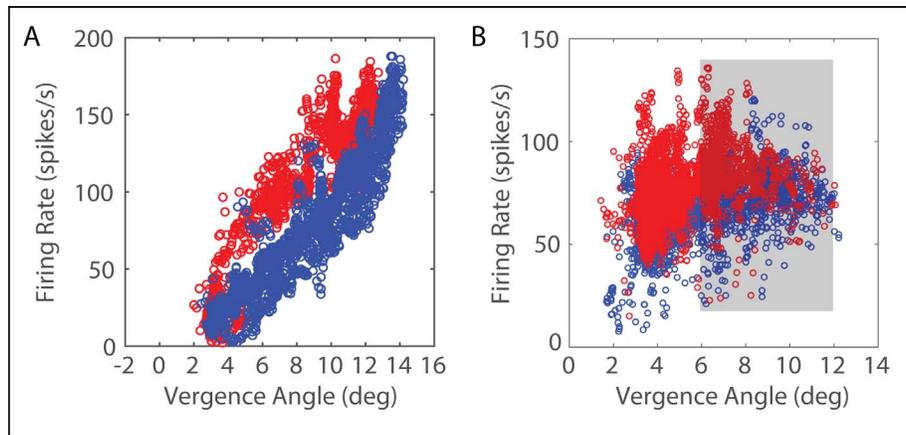
FIGURE 5. Relationship between instantaneous firing rate and vergence angle for two example near response cells, recorded from monkey CI during performance of the smooth vergence tracking task in a lighted room, under binocular viewing conditions, with the target surrounded by a full-field checkerboard pattern. Data obtained during the convergence phase (target approaching the monkey) are shown in *red*; data obtained during the divergence phase are shown in *blue* (target receding from the monkey). For the neuron in panel **A**, firing rate increased monotonically with vergence angle; for the neuron shown in panel **B**, the firing rate reached a plateau at approximately 4° to 6° convergence, even though the monkey was able to achieve vergence angles of >10°. However, the firing rate declined slightly over the range of 6° to 12° convergence (*rectangle*).

while the monkey unsuccessfully attempted to perform the task without the checkerboard pattern.

In this task, the target velocity in external space is constant during approach, but the relationship between target distance and the required vergence angle is nonlinear (see companion paper). For this reason, successful performance of this task requires a nonlinear increase in vergence velocity as the target nears. With this in mind, one might expect the firing rate of an SOA neuron that is sensitive to both vergence position and velocity to increase more rapidly as vergence angle increases. Figure 5 shows the relationship between firing rate and vergence angle during convergence (red) and divergence (blue), for two near response cells. For the near response cell shown in panel A, the firing rate increases monotonically as the monkey converges. Note that the firing rate for a given vergence position varies, depending on whether the monkey is converging or diverging, indicating a robust sensitivity to vergence velocity. One can see a very different effect for the neuron shown in panel B. For this near response cell, the firing rate increases up to approximately 6° convergence but then saturates; there is no further increase even though the vergence angle reaches 12°. Thus, there is a clear deviation from nonlinearity, but it is in the opposite direction from what one might expect. That is, the firing rate increases more rapidly when the vergence velocity is low and more slowly when the vergence velocity is high.

Equation 4 was used to estimate the vergence position and velocity sensitivities of all 11 neurons recorded during performance of the smooth vergence tracking task. Overall, the estimated vergence position sensitivities were better than what we observed during performance of the near fixation task. The mean absolute value for these 11 neurons was 7.79. These dynamic model fits were quite good for 4/11 neurons (R^2, >0.65), including the neuron shown in Figure 5A. The estimated vergence position sensitivities were >10 for all four of these cells. For all of the remaining seven neurons, the fits were poor (R^2, <0.20 for all). The reason for this is apparent in Figure 5B, specifically the nonlinearity for convergence ~>6°. Note that the firing rates begin to decline slightly as vergence angle increases from 6° to 12°. Indeed, when the same model was used to fit the data for vergence angles >6°, the vergence position slopes were negative over this range for two near response cells, even though the overall static vergence position

sensitivities for these neurons were positive. For another two of these cells, the estimated vergence position sensitivities were <0.5 for convergence >6°.

DISCUSSION

In the companion paper, we reported behavioral data from a rhesus monkey with a naturally occurring impairment of vergence eye movements. In the present paper, we have shown that near and far response cells in the SOA show reduced slopes for vergence rate-position curves in this same animal, compared to normal monkeys. Linear fits to this relationship yielded smaller slopes and reduced R^2 values, compared to previously published data from normal monkeys.[8] Similarly, for vergence-only movements, the vergence velocity sensitivity was notably weaker than what has been reported for SOA neurons in normal monkeys in previous studies (present study = 0.31; Pallus et al.[8] = 1.12; Mays et al.[4] = 0.71). This indicates a serious abnormality, either in the vergence circuits themselves or in the sensory signals that drive vergence eye movements.

In the companion paper, we saw that enriching the number and robustness of visual depth cues led to a large improvement in this animal's performance on vergence tasks. Normal subjects also show improved performance on vergence tasks when more cues are available, but monkey CI's improvement was quite large. When the animal was presented with a sufficiently rich array of cues (disparity, accommodative blur, looming, and radial optic flow), he was able to achieve a reasonably normal performance on the smooth vergence tracking task, and a subset of SOA neurons showed a robust modulation. Similarly, the vergence rate-position curves were highly variable, with some neurons showing robust modulation (see Fig. 1). Zhang et al.[6] used a display system that dissociated vergence and accommodation and reported that individual SOA neurons can be sensitive to one or the other or a combination of the two. We speculate that our SOA neurons that showed poor sensitivity were those that were driven primarily by sensory input that, in this animal, is disturbed (i.e., disparity).

It should be noted that the abnormally small slopes in our study mean that a relatively small increase in firing rate is associated with an unexpectedly large change in vergence

angle. This may point to a compensatory process that maximizes the convergence that can be achieved, given inadequate drive to the vergence system. In recent years, the authors of some studies have suggested a distinction between slow and fast vergence.[20–23] Consistent with this idea, we have recently shown that when normal monkeys perform our saccade-vergence task, SOA neurons encode the slow vergence changes but do not discharge at a high enough rate to account for the fast intrasaccadic vergence.[8] In one of their models of saccade-vergence interactions, Zee et al.[24] postulated the existence of a separate population of "saccade-related vergence burst neurons" that would exhibit a burst of spikes during fast vergence but would be quiescent during conjugate saccades or slow vergence. If there is a functional distinction between slow and fast vergence, it is possible that monkey CI relies more heavily on the latter when attempting to converge to a near target. That might explain the slow divergence drift that often begins immediately following converging saccades in this animal. The present data suggest that these inappropriate slow divergence movements may not be encoded by SOA neurons. Instead, we propose that they result from an inability to properly coordinate slow and fast vergence. The monkey repeatedly makes converging saccades to achieve vergence angles that the slow vergence system is unable to fully maintain (see Fig. 1). This leads to difficulty maintaining sensory fusion, which sometimes causes the monkey to "give up," making voluntary divergence-only movements that are encoded by SOA neurons (Fig. 1B).

Acknowledgments

References

1. Trieu LH, Lavrich JB. Current concepts in convergence insufficiency. *Curr Opin Ophthalmol* 2018;29:401–406.

2. Mays LE. Neural control of vergence eye movements: convergence and divergence neurons in midbrain. *J Neurophysiol*. 1984;51:1091–1108.

3. Judge SJ, Cumming BG. Neurons in the monkey midbrain with activity related to vergence eye movement and accommodation. *J Neurophysiol*. 1986;55:915–930.

4. Mays LE, Porter JD, Gamlin PD, Tello CA. Neural control of vergence eye movements: neurons encoding vergence velocity. *J Neurophysiol*. 1986;56:1007–1021.

5. Pallus AC, Walton MMG, Mustari MJ. Activity of near response cells during disconjugate saccades in strabismic monkeys. *J Neurophysiol*. 2018;120:2282–2295.

6. Zhang Y, Mays LE, Gamlin PD. Characteristics of near response cells projecting to the oculomotor nucleus. *J Neurophysiol*. 1992;67:944–960.

7. Mays LE, Gamlin PD. Neuronal circuitry controlling the near response. *Curr Opin Neurobiol*. 1995;5:763–768.

8. Pallus AC, Walton MMG, Mustari MJ. Response of supra-oculomotor area neurons during combined saccade-vergence movements. *J Neurophysiol*. 2018;119:585–596.

9. Mustari MJ, Tusa RJ, Burrows AF, Fuchs AF, Livingston CA. Gaze-stabilizing deficits and latent nystagmus in monkeys with early-onset visual deprivation: role of the pretectal not. *J Neurophysiol*. 2001;86:662–675.

10. Ono S, Mustari MJ. Horizontal smooth pursuit adaptation in macaques after muscimol inactivation of the dorsolateral pontine nucleus (DLPN). *J Neurophysiol*. 2007;98:2918–2932.

11. Walton MM, Ono S, Mustari MJ. Stimulation of pontine reticular formation in monkeys with strabismus. *Invest Ophthalmol Vis Sci*. 2013;54:7125–7136.

12. Fuchs AF, Robinson DA. A method for measuring horizontal and vertical eye movement chronically in the monkey. *J Appl Physiol*. 1966;21:1068–1070.

13. Judge SJ, Richmond BJ, Chu FC. Implantation of magnetic search coils for measurement of eye position: an improved method. *Vis Res*. 1980;20:535–538.

14. Walton MM, Mustari MJ, Willoughby CL, McLoon LK. Abnormal activity of neurons in abducens nucleus of strabismic monkeys. *Invest Ophthalmol Vis Sci*. 2014;56:10–19.

15. Walton MM, Mustari MJ. Abnormal tuning of saccade-related cells in pontine reticular formation of strabismic monkeys. *J Neurophysiol*. 2015;114:857–868.

16. Walton MM, Ono S, Mustari M. Vertical and oblique saccade disconjugacy in strabismus. *Invest Ophthalmol Vis Sci*. 2014;55:275–290.

17. Kodaka Y, Sheliga BM, FitzGibbon EJ, Miles FA. The vergence eye movements induced by radial optic flow: some fundamental properties of the underlying local-motion detectors. *Vis Res*. 2007;47:2637–2660.

18. Busettini C, Masson GS, Miles FA. Radial optic flow induces vergence eye movements with ultra-short latencies. *Nature*. 1997;390:512–515.

19. Inoue Y, Takemura A, Suehiro K, Kodaka Y, Kawano K. Short-latency vergence eye movements elicited by looming step in monkeys. *Neurosci Res*. 1998;32:185–188.

20. Van Horn MR, Waitzman DM, Cullen KE. Vergence neurons identified in the rostral superior colliculus code smooth eye movements in 3D space. *J Neurosci*. 2013;33:7274–7284.

21. Van Horn MR, Cullen KE. Dynamic coding of vertical facilitated vergence by premotor saccadic burst neurons. *J Neurophysiol*. 2008;100:1967–1982.

22. Van Horn MR, Sylvestre PA, Cullen KE. The brain stem saccadic burst generator encodes gaze in three-dimensional space. *J Neurophysiol*. 2008;99:2602–2616.

23. King WM, Zhou W. Neural basis of disjunctive eye movements. *Ann NY Acad Sci*. 2002;956:273–283.

24. Zee DS, Fitzgibbon EJ, Optican LM. Saccade-vergence interactions in humans. *J Neurophysiol*. 1992;68:1624–1641.